Nonlinear constrained predictive control applied to a coupled-tanks apparatus

N.K.Poulsen, B.Kouvaritakis and M.Cannon

Abstract: The focus of the paper is the development and application to experimental equipment of fast constrained predictive control algorithms based on feedback linearisation. Rather than use quadratic programming (QP) optimisation is performed, deploying a computationally much cheaper alternative based on interpolation and linear programming (LP). Despite its undemanding computational nature, this algorithm is found to perform well both in simulation, and when applied to an actual couple-tanks rig. The advantages of the algorithm are further illustrated by comparison with PID control.

1 Introduction

From the early stages [1, 2] and especially after its later development [3, 4] predictive control has attracted a great deal of interest both in industry and academia. Various properties of predictive strategies have been addressed by a large number of authors, whereas issues of stability have formed the main focus of more recent papers, e.g. [5] and [6]. One of the reasons for the popularity of predictive control is that its receding horizon implementation allows for the systematic handling of hard constraints on system inputs and states [7–11]. In connection to hard constraints on inputs there exist several methods such as anti-windup and signal conditioning. In [12] it is shown that there is a close relationship between handling input constraints using anti-windup and predictive control. In this paper, we focus on constraints on both system states and inputs. The conventional tool used in this context is quadratic programming (QP) which may be computationally very demanding and therefore is more suitable for applications with relatively slow sampling rates. Suboptimal solutions offer the means of significant reduction in the computational load, and the trade-off between closed-loop dynamic performance and computational complexity forms an issue of practical importance [13–15].

This is the perspective adopted in this paper which examines strategies that deploy one-dimensional linear programming (LP) rather than QP as the basic optimisation tool. An interpolation technique involving unconstrained optimal trajectories is used to reduce the degree of suboptimality, while of course still retaining the computational advantages. The efficacy of this approach is illustrated in terms of experimental results obtained on a laboratory rig where it is compared with a PID controller with desaturation and bumpless transfer described. The emphasis in this paper is on ease of computation rather than the complexity of the systems that can be controlled by the algorithm. However, the performance of the algorithm is evaluated when connected to a real laboratory rig.

IEE Proceedings online no. 20010231

DOI: 10.1049/ip-cta:20010231

Paper first received 8th February and in revised form 5th October 2000

N.K. Poulson is with the Department of Mathematical Modelling, Technical University of Denmark, Building 321, DK-2800 Kgs., Lyngby, Denmark

B. Kouvaritakis and M. Cannon are with the Department of Engineering Science, University of Oxford, Parks Road, Oxford, OX1 3PJ, UK

2 The coupled tanks system

The apparatus, see Fig. 1, consists of two coupled tanks with an inlet from a variable speed pump into the first tank and an outlet from the second. The two tanks are connected through a pipe. The objective of the control problem is to adjust the inlet flow q so as to maintain the level in the second tank, h_2 as close to a desired set point, w. Sensors measure the levels h_1 and h_2 in the two tanks.

The dynamics of the system are modelled by the state-space model equations:

$$C\dot{h}_1 = q - q_1 \qquad C\dot{h}_2 = q_1 - q_2 \tag{1}$$

where the flows obey Bernoulli's equation, i.e.

$$q_1 = \sigma_l a_l \sqrt{2g(h_1 - h_2)} \quad \text{for} \quad h_1 \geq h_2$$

$$q_2 = \sigma_o a_o \sqrt{2gh_2} \quad \text{for} \quad h_2 \geq 0$$

The output equation for the system is

$$y = h_2$$

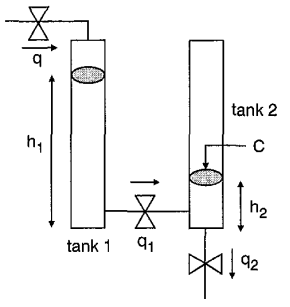

Fig. 1 *Coupled-tanks apparatus*
$a_o = 0.8$ cm^2 $a_l = 0.5$ cm^2 $c = 153.9$ cm^2
$q_2 = \sigma_o a_o \sqrt{(2gh_2)}$ for $h_2 \geq 0$

The cross-section area is determined from the diameter of the tanks and the orifice constants have experimentally (from steady-state measurements) been determined to be $\sigma_i = 0.49$ and $\sigma_o = 0.153$.

Several constraints have to be considered. Limited pump capacity implies that values of q range from 0 to 96.3 cm^3/s. The limits for both levels, h_1 and h_2 are 0 cm and 60 cm.

3 Feedback linearisation

The system model in eqn. 1 is nonlinear, but the nonlinearities are smooth and the model has a full relative degree. We will apply the feedback linearisation method, shown in Fig. 2 which is described in more detail in the Appendix (Section 11.1). Feedback linearisation cannot be applied to systems with unstable zero dynamics, but this is not a problem here owing to the fact that the system has a full relative degree.

Let

$$\boldsymbol{h} = \begin{bmatrix} h_1 \\ h_2 \end{bmatrix}$$

and let $\boldsymbol{x}$ be a vector with same dimension. Use of the mapping $\boldsymbol{x} = \varphi(\boldsymbol{h})$ (which can be proven to be a smooth bijective mapping with a smooth inverse) and the feedback linearisation $q = \psi(u, \boldsymbol{h})$, renders linear dynamics from input control u to output y. For the coupled-tanks system the mapping

$$\varphi(\boldsymbol{h}) = \begin{bmatrix} h_2 \\ -a_1\sqrt{h_2} + a_2\sqrt{h_1 - h_2} \end{bmatrix} \tag{2}$$

and the feedback linearisation

$$\psi(u, \boldsymbol{h}) = (\alpha_1 u_t + \alpha_2)\sqrt{h_1 - h_2} + \alpha_3\left(\frac{h_1 - h_2}{h_2} - 1\right)\sqrt{h_2} \tag{3}$$

brings the description into the linear form

$$\begin{bmatrix} \dot{x}_1 \\ \dot{x}_2 \end{bmatrix} = \begin{bmatrix} 0 & 1 \\ 0 & 0 \end{bmatrix}\begin{bmatrix} x_1 \\ x_2 \end{bmatrix} + \begin{bmatrix} 0 \\ \beta \end{bmatrix} u \tag{4}$$

$$y = [1\ 0]\begin{bmatrix} x_1 \\ x_2 \end{bmatrix}$$

where the constants β, a_i, $i = 1, 2$ and α_i, $i = 1, 2, 3$ are given in the Appendix (Section 11.1). For brevity the system, given by eqn. 4 will be denoted as the continuous time FBL system. It is noticed that as a result of the feedback linearisation, x_2 is the derivative of the output $y = x_1$. The inverse mapping of eqn. 2 is given by

$$\begin{bmatrix} h_1 \\ h_2 \end{bmatrix} = \phi(\boldsymbol{x}) = \begin{bmatrix} \left(\dfrac{x_2 + a_1\sqrt{x_1}}{a_2}\right)^2 + x_1 \\ x_1 \end{bmatrix} \tag{5}$$

The algorithm is implemented on a PC. Consequently, feedback linearisation eqn. 3, which is inherently in continuous time, must be approximated in discrete time. This is simply done by using a sampling frequency, which is much higher than the closed-loop bandwidth. The choice $t_s = 1$ s is considered adequate, when compared to the closed–loop rise time of approximate 5 min.

4 Unconstrained control

Sampling the FBL system with 0.2 Hz we obtain a linear description in discrete time. (Notice the digital realisation of the feedback linearisation is obtained with 1 Hz, whereas thc control of the FBL system is done with 0.2 Hz). However, approximation errors in the model (as well as possible disturbances) necessitate the use of integral action, Fig. 3, which for a reference signal, w can be implemented by:

$$z_{t+1} = z_t + w_t - y_t$$

and can be introduced in the model dynamics by augmenting the state vector

$$\begin{bmatrix} x \\ z \end{bmatrix}_{t+1} = \begin{bmatrix} \boldsymbol{A} & 0 \\ -\boldsymbol{C} & 1 \end{bmatrix}\begin{bmatrix} \boldsymbol{x} \\ z \end{bmatrix}_t + \begin{bmatrix} \boldsymbol{B} \\ 0 \end{bmatrix} u_t + \begin{bmatrix} 0 \\ 1 \end{bmatrix} w_t \tag{6}$$

$$y_t = (\boldsymbol{C}\ 0)\begin{bmatrix} \boldsymbol{x} \\ z \end{bmatrix}_t$$

The matrices $\boldsymbol{A}$, $\boldsymbol{B}$ and $\boldsymbol{C}$ are obtained from eqn. 4. The cost function, which now must include a term that penalises deviations of the integrator state z from its equilibrium z^0, can be written as:

$$J_t = \sum_{k=t}^{\infty}\begin{bmatrix} \boldsymbol{x}_k - \boldsymbol{x}_k^0 \\ z_k - z_k^0 \end{bmatrix}^T \boldsymbol{Q}\begin{bmatrix} \boldsymbol{x}_k - \boldsymbol{x}_k^0 \\ z_k - z_k^0 \end{bmatrix} + R(u_k - u_k^0)^2 \tag{7}$$

The values $\boldsymbol{Q} = \mathrm{diag}(1\ 1\ 1)$ and $R = 0.01$ are used in the results shown later, and yield the optimal feedback gain

$$\boldsymbol{L} = [77\ 1663\ -7.92]$$

Since integral action is included in the control loop, the equilibrium values in the cost function are not needed in the control law. Let for short

$$\underline{\boldsymbol{x}}_t = \begin{bmatrix} \boldsymbol{x} \\ z \end{bmatrix}_t$$

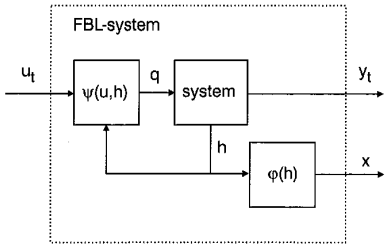

Fig. 2 *Feedback linearised system*

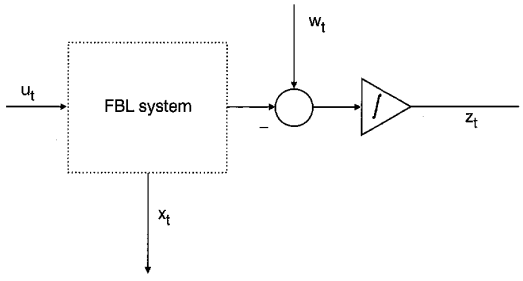

Fig. 3 *Feedback linearised (FBL) system with integral action*

The cost function has an unconstrained minimum for

$$u_k = Mw_k - \boldsymbol{L}\underline{\boldsymbol{x}}_k$$

which, owing to the fact that the output is the first element of the state vector, implies that the feed-forward term M is equal to the first element of $\boldsymbol{L}$. The optimal cost function achieves the value

$$J_t^* = \underline{\tilde{\boldsymbol{x}}}_t^T S \underline{\tilde{\boldsymbol{x}}}_t \quad \text{where} \quad \underline{\tilde{\boldsymbol{x}}} = \underline{\boldsymbol{x}}_t - \underline{\boldsymbol{x}}_t^0$$

and where $\boldsymbol{S}$ is obtained from the Ricatti equation associated with the optimal control problem defined by eqns. 6 and 7.

5 Constrained predictive control

The objective is to control the level in tank 2 in such a manner that the cost function in eqn. 7 is minimised subject to the constraints

$$\begin{aligned} 0\,\text{cm}^3/\text{s} \le\ & q \le 96.3\,\text{cm}^3/\text{s} \\ 0\,\text{cm} \le\ & h_1 \le 60\,\text{cm} \\ 0\,\text{cm} \le\ & h_2 \le 60\,\text{cm} \end{aligned} \tag{8}$$

The method applied in this paper is based on receding predictive control of the sampled version of the augmented FBL system in eqn. 6. The constraints are included in the problem by applying thc interpolation technique described in the Appendix (Section 11.2) and referred to as Suboptimal constrained predictive control (SCPC). Here, however, the perturbation of the unconstrained control law, is carried out as a perturbation, v_t, on the set point, i.e.

$$u_l = M(w_l + v_l) - L\underline{\boldsymbol{x}}_t \tag{9}$$

At time t the predicted states and control input to the FBL-system can be determined through

$$\underline{\hat{\boldsymbol{x}}}_{k+1|t} = \Phi \underline{\boldsymbol{x}}_{k|t} + \Gamma \tilde{w}_{k|t} \tag{10}$$

where

$$\Phi = \begin{bmatrix} \boldsymbol{A} - \mathbf{B}\mathbf{L}_x & -\boldsymbol{B}L_z \\ -\boldsymbol{C} & 1 \end{bmatrix} \qquad \Gamma = \begin{bmatrix} \boldsymbol{B}M \\ 1 \end{bmatrix}$$

Furthermore

$$\hat{u}_{k|t} = M\tilde{w}_{k|t} - \boldsymbol{L}\begin{bmatrix} \hat{\boldsymbol{x}} \\ \hat{z} \end{bmatrix}_{k|t} \tag{11}$$

where $\tilde{w}_{k|t} = w_k + \hat{v}_{k|t}$ is the perturbed set point and $k \ge t$ is a future instant of time. $\boldsymbol{L}_x$ and L_z are the feedback gain from $\boldsymbol{x}$ and z, respectively. Note that the fast matrix techniques deployed in the Appendix (Section 11.2) can also be applied here for determining the prediction of x and u, which are the state vector and the control input to the FBL system and are, of course, not the actual constrained variables.

Let the extension to the current time of the previously planned perturbation $\hat{v}_{k|t-1}$ be referred to as the tail which, by definition, results in feasible trajectories. At each instant of time t we perform a linear interpolation between the tail and the unconstrained state feedback law, which is obtained for $\hat{v}_{k|t} = 0$. Since the cost function can be written as

$$J_t = \underline{\tilde{\boldsymbol{x}}}_t^T S \underline{\tilde{\boldsymbol{x}}}_t + \sum_{k=t}^{\infty} \hat{v}_{k|t}^T \sigma_c \hat{v}_{k|t} \tag{12}$$

($\sigma_c > 0$) and since the interpolation

$$\hat{v}_{k|t} = \alpha_t \hat{v}_{k|t-1} \tag{13}$$

is linear, we have to find the smallest value of $0 \le \alpha_t \le 1$ which results in feasible trajectories. In the Appendix (Section 11.2) this is shown to be a very simple scalar LP problem. However, here the relations between the states and control inputs to the FBL-system and the actual quantities ($\boldsymbol{h}$ and q) in expr. 8 are given through the nonlinear functions $\phi(\boldsymbol{x}) = \varphi^{-1}(x)$ and $\psi(u, \boldsymbol{h})$. Consequently, we have to apply numerical but simple (well known) univariate procedures, e.g. bisection etc., to solve this nonlinear problem. In a little more detail, we have to minimise α_t subject to $0 \le \alpha_t \le 1$ and such that the trajectories $\hat{\boldsymbol{h}}_{k|t}$ and $\hat{q}_{k|t}$ satisfy the constraints of expr. 8. Let the matrices Φ and Γ be as given in eqn. 10 From eqn. 10 we (for $k = t + \kappa$, $\kappa \ge 0$) have

$$\begin{aligned} \underline{\hat{\boldsymbol{x}}}_{k|t} &= \Phi^{\kappa} \underline{\boldsymbol{x}}_t + C_{\kappa}(\boldsymbol{W} + \alpha_t \boldsymbol{V}) \\ \mathbf{W} &= \begin{bmatrix} w_t \\ \vdots \\ w_k \end{bmatrix} \quad \mathbf{V} = \begin{bmatrix} \hat{v}_{t|t-1} \\ \vdots \\ \hat{v}_{k|t-1} \end{bmatrix} \end{aligned} \tag{14}$$

which for

$$C_h = [\Phi^{\kappa-1}\Gamma, \ldots, \Gamma, 0]$$

is a linear interpolation in α_t. Additionally, from eqn. 11 we have that

$$\hat{u}_{k|t} = M(w_k + \alpha_t \hat{v}_{k|t-1}) - \boldsymbol{L}\underline{\hat{\boldsymbol{x}}}_{k|t} \tag{15}$$

is also a linear interpolation in α_t. However, since ϕ and ψ in

$$\hat{\boldsymbol{h}}_{k|l} = \phi(\underline{\hat{\boldsymbol{x}}}_{k|t}) \qquad \hat{q}_{k|t} = \psi(\hat{u}_{k|t}, \hat{\boldsymbol{h}}_{k|t}) \tag{16}$$

are nonlinear functions, the optimisation problem is no longer a simple LP problem as described in the Appendix (Section 11.2), but a univariate minimisation of α_t ($0 \le \alpha_t \le 1$) such that the predicted trajectories satisfy expr. 8.

SCPC is based on the existence of an initial perturbation, $v_{k|0}$, which results in feasible trajectories. Owing to the fact that a reduction in the activity in u_t implies reduced activities in q_t and h_t, the initial perturbation, $v_{k|0}$, can be found as the one that minimises

$$J = \sum_{k=0}^{\infty} \underline{\boldsymbol{x}}_t^T \underline{\boldsymbol{Q}} \underline{\boldsymbol{x}}_t + v_t^T \underline{R} v_t$$

subject to the system dynamic

$$\begin{aligned} \underline{\boldsymbol{x}}_{t+1} &= \Phi \underline{\boldsymbol{x}}_t + \Gamma v_t \\ u_t &= -\boldsymbol{L}\underline{\mathbf{x}}_t + v_t \end{aligned}$$

for a value of $\underline{\boldsymbol{x}}_0$ which reflects the size of the setpoint change, i.e. $\underline{\boldsymbol{x}}_0$ has to be proportional to the size of the change. The values $\underline{\boldsymbol{Q}} = \text{diag}(0.1,\ 0.1,\ 0.1)$ and $\underline{R} = 0.1$ were applied in the experiments shown in Section 7.

6 Desaturated PID control

For the purpose of comparison, the tank apparatus is also controlled with a PID controller equipped with desaturation, see Fig. 4. Desaturated PID has been chosen owing to its status as a standard method used in the control of many industrial constrained applications. The PID controller was realised with a sampling period $t_s = 1$ s, which corresponds

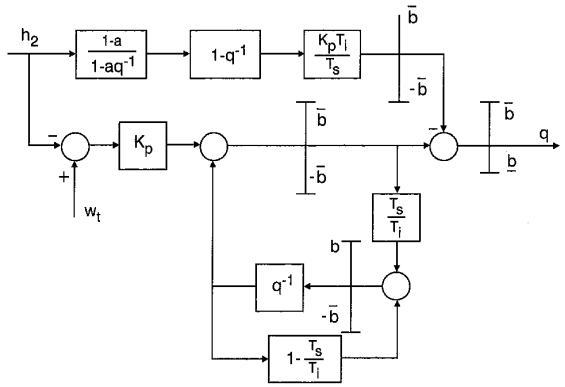

Fig. 4 *Digital PID-controller with desaturation*
q^{-1} is the delay operator

to the discrete-time approximation of the feedback linearisation. The constants used in the experiments were

$$K_p = 20\,\text{cm}^2/\text{s} \quad T_d = 20\,\text{s} \quad T_i = 50\,\text{s}$$

$$\bar{b} = 96.3\,\text{cm}^3/\text{s} \quad \underline{b} = 0\,\text{cm}^3/\text{s} \quad a = 0.97$$

Note that the measurement of the level in tank 2 is low-pass filtered before it is used in the D-part of the PID controller.

7 Results

Three experiments, E_1, E_2 and E_3 have been carried out. In both E_1 and E_2 the set point is changed from 20 cm to 40 cm and back and a comparison is drawn between SCPC(E_1) and PID(E_2). The QP-based optimal constrained predictive control, LQCPC, see the Appendix (Section 11.2) is not applied owing to the fact that the computational demands of the LQCPC could not be met with our limited power within the chosen sampling interval of 5 s. SCPC is also applied in E_3, in which the set point is changed from 35 cm to 45 cm and back.

Fig. 5 shows the level in tank 2 (output, y), the set point (w) and the perturbed set point ($w+v$) for the first experiment (E_1). Fig. 6 shows the inflow q obtained in the same experiment.

For the purpose of comparison the same experiment was carried out with the desaturated PID controller. The results are shown in Figs. 7 and 8. Clearly, the simple SCPC produced good responses which outperformed PID control. Note that the overshoot is smaller and more symmetric in the first experiment. This is due to the fact that predictive control with feedback linerisation takes explicit account of the nonlinearities in the system dynamics. The inflow is smoother in the second experiment owing to the low-pass filter in the PID controller. In the SCPC, the levels are measured directly without any filtration. A Kalman filter might have reduced the effect from the measurements noise.

In the two first experiments, the limitation on the pump capacity is the only active constraint. In order to make sure that the level constraints also play an active role, the set point must be chosen to be higher and hence, in the third experiment E_3, they were chosen to be 35 cm and 45 cm. The results are shown in Fig. 9–11. From Fig. 11 it is obvious that the limited pump capacity is active immediately after the set-point change. After a short while the upper tank limit takes over. Again the SCPC performed

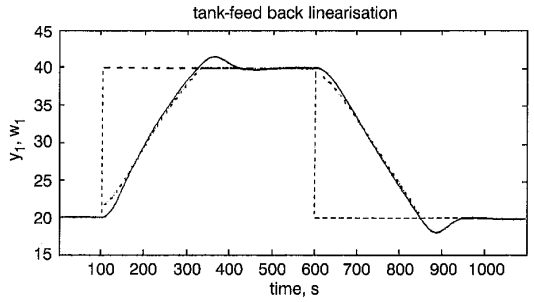

Fig. 5 *Output ($y_t = h_2$), set point (w_t) and modified set point ($w_t + v_t$) obtained with SCPC in E_1*
—— y_t
· – · $w_t + v_t$
– – w_t

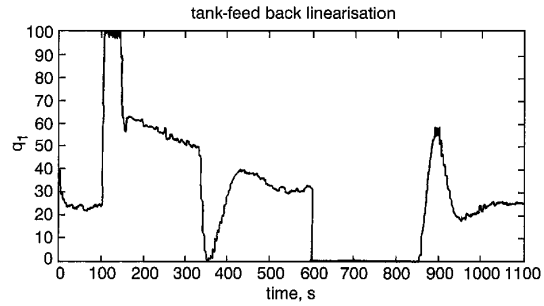

Fig. 6 *Inflow (q) obtained with SCPC in E_1*
—— q_t

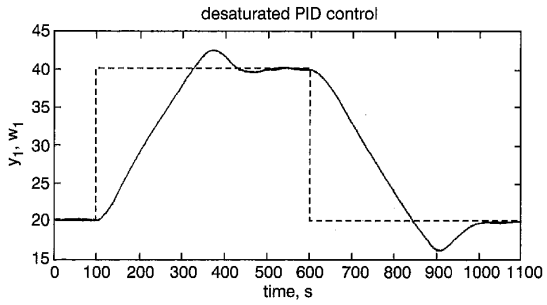

Fig. 7 *Output and set point obtained in E_2 with desaturated PID control*
—— y_t
– – w_t

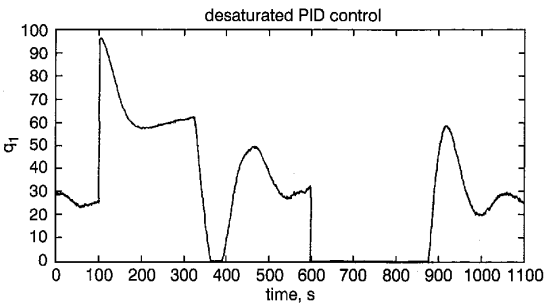

Fig. 8 *Control input (inflow) obtained in E_2 with desaturated PID control*
—— q_t

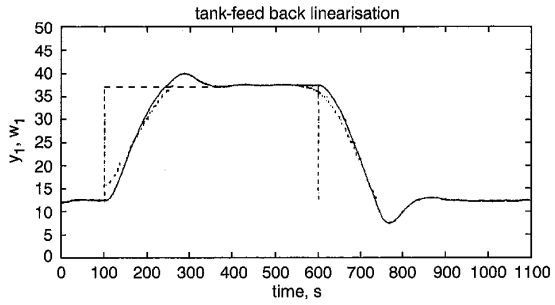

Fig. 9 *Output, set point and perturbed set point obtained with SCPC in E_3*
—— y_t
· – · $w_t + v_t$
– – – w_t

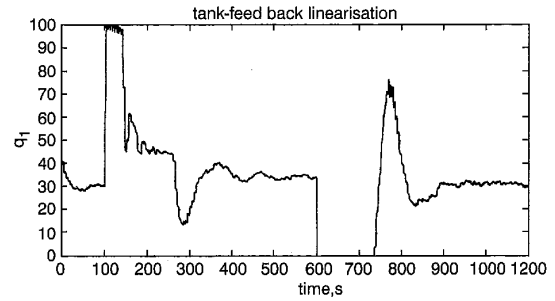

Fig. 10 *Inflow obtained with SCPC in E_3*
—— q_t

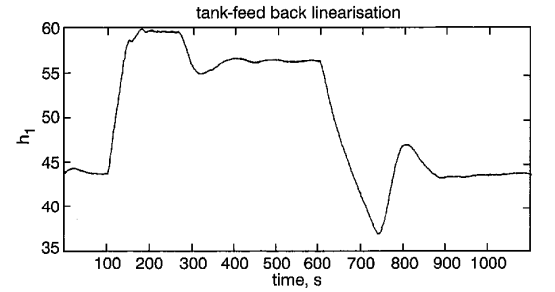

Fig. 11 *Level (h_1) in the first tank obtained with SCPC in E_3*
—— h_1

well: indeed the quality of control is comparable to that obtained in E_1.

8 Conclusion

The focus of this paper is the development of constrained predictive control and its application to a coupled-tanks apparatus. This system is known to be a nonlinear system with soft nonlinearities. The constraints consist of limitations on the levels in the tanks and on the control input.

The nonlinearities are handled by applying a predictive control algorithm which is based on feedback linearisation. One of the reasons for the popularity of predictive control is that its receding horizon implementation allows for the systematic handling of hard constraints on both system inputs and states. Earlier work proposed LQ-based predictive control algorithms which, for the nominal case, can produce optimal results. This advantage is gained at a considerable computational expense which reduces the applicability of the approach. Interpolation between feasible and unconstrained optimum trajectories provides a sensible way of sacrificing some degree of optimality for a very considerable reduction in computational cost.

The described algorithm is applied to an actual laboratory rig and its ability to cope with constraints in the control input are compared to that of a desaturated PID controller. The predictive controller performs well and gives better results than the PID controller. The predictive controller is also applied in a situation with active level constraints. Again, the predictive controller produces good responses and prevents flooding.

9 Acknowledgment

Support from the Engineering and Physical Research Council, UK and the Danish Research Council for Technical Science (under grant 9800576) is gratefully acknowledged.

10 References

1 RICHALET, J., RAULT, A., TESTUD, J.L., and PADON, J.: 'Model predictive heuristic control: application to industrial processes', *Automatica*, 1978, **14**, pp. 413–428
2 CUTLER, C.R., and RAMAKER, B.L.: 'Dynamic matrix control—a computer control algorithm'. Proceedings of the *Joint automatic control* Conference, 1980
3 CLARKE, D.W., MOHTADI, C., and TUFFS, P.S.: 'Generalized predictive control—part I: the basic algorithm', *Automatica*, 1987, **23**, (2), pp. 137–148
4 CLARKE, D.W., MOHTADI, C., and TUFFS, P.S.: 'Generalized predictive control—part II: extentions and interpretations', *Automatica*, 1987, **23**, (2), pp. 149–160
5 CLARKE, D.W., and SCATTOLINI, R.: 'Constrained receding-horizon predictive control', *IEE Proc. D, Control Theory Appl.*, 1991, **138**, (4), pp. 347–354
6 KOUVARITAKIS, B., ROSSITER, J.A., and CHANG, A.O.T.: 'Stable generalised predictive control: an algorithm with guaranteed stablility', *IEE Proc. D, Control Theory Appl.*, 1992, **139**, (4), pp. 349–362
7 KOUVARITAKIS, B., ROSSITER, J.A., and CANNON, M.: 'Linear quadratic feasible predictive control', *Automatica*, 1998, **34**, (12), pp. 1583–1592
8 SCOKAERT, P.O.M., and RAWLINGS, J.B.: 'Infinite horizon linear quadratic control with constraints'. Proceedings of the IFAC World Congress, San Francisco, USA, number 1 in 7a-04, pp. 109–114, 1996
9 SCOKAERT, P.O.M., and RAWLINGS, J.B.: 'Constrained linear quadratic regulation.', *IEEE Trans. Autom. Control*, 1998, **43**, (8), pp. 1163–1169
10 SCOKAERT, P.O.M., and MAYNE, M.Q.: 'Min-max feedback model predictive control for constrained linear systems', *IEEE Trans. Autom. Control*, 1998, **43**, (8), pp. 1136–1142
11 ROSSITER, J.A., RICE, M.J., and KOUVARITAKIS, B.: 'A robust state-space approach to stable predicitve control strategies'. In Proceedings of the *American Control* Conference (ACC97), Albuquerque, New Mexico, USA, **3**, pp. 1640–1641, AACC, 1997
12 DE DONA, J.A., GOODWIN, G.C., and SCRON, M.M: 'Connection between model predictive control and anti-windup strategies for dealing with saturation actuators'. Proceedings of the *European Control* Conference ECC99, 1999
13 CANNON, M.: 'Constrained predictive control'. 1998, PhD thesis, Department of Engineering Science, University of Oxford
14 CANNON, M., and KOUVARITAKIS, B.: 'Fast suboptimal predictive control with guaranteed stability', *Syst. Control Lett.*, 1998, **35**, pp. 19–29
15 KOUVARITAKIS, B., CANNON, M., and ROSSITER, J.A.: 'Stability, feasibility, optimality and the degrees of freedom in constrained predictive control *in* ALLGOWER, F., and ZHENG, A. (Eds.): 'Nonlinear model predictive control' (Birkhäuser-Verlag, 2000)
16 SLOTINE, J.E., and LI, W.: 'Applied nonlinear control' (Prentice Hall, 1991)
17 ISIDORI, A.: 'Nonlinear control systems' (Springer-Verlag, New York Inc., 1980)
18 ROSSITER, J.A., KOUVARITAKIS, B., and RICE, M.J.: 'A numerically robust state-space approach to stable-predictive control strategies', *Automatica*, 1998, **34**, (1), pp. 65–73

11 Appendix

11.1 Feedback Linearization

This Appendix gives a short review of feedback linearisation cf. [16, 17], as applied to the coupled-tanks system.

Let

$$z_1 = h_2 \quad z_2 = h_1 - h_2 \quad \text{and} \quad z = \begin{bmatrix} z_1 \\ z_2 \end{bmatrix}$$

Then the model in eqn. 1 can easily be expressed as

$$\dot{z} = f(z) + g(z)q$$
$$y = c(z)$$

where for

$$a_1 = \frac{\sigma_o a_o \sqrt{2g}}{C} \quad a_2 = \frac{\sigma_l a_l \sqrt{2g}}{C}$$

$$\begin{bmatrix} \dot{z}_1 \\ \dot{z}_2 \end{bmatrix} = \begin{bmatrix} -a_1 & a_2 \\ a_1 & -2a_2 \end{bmatrix} \begin{bmatrix} \sqrt{z_1} \\ \sqrt{z_2} \end{bmatrix} + \begin{bmatrix} 0 \\ \frac{1}{C} \end{bmatrix} q$$

$$y = z_1$$

Here f, g and c are smooth vector fields in $\mathcal{S} = \{(z_1, z_2) \in \mathbb{R}^2 | z_1 > 0, z_2 > 0\}$, which is the normal area of operation for the tanks apparatus. Furthermore, it is easily verified that the system has a relative degree $r = n$ (where $n = 2$) at every point in $\mathcal{S}$. Then there exists a diffeomorphism $\boldsymbol{x} = \varphi_z(z)$ in $\mathcal{S}$,

$$\varphi_z(z) = \begin{bmatrix} c(z) \\ \vdots \\ L_f^{r-1} c(z) \end{bmatrix}$$

and a feedback law $q = \psi_z(u, z)$

$$\psi_z(u, z) = \frac{u - L_f^r c(z)}{L_g L_f^{r-1} c(z)}$$

where e.g. $L_f c$ is the Lie derivative of c with respect to f, such that the dynamic maps from u to y are given by

$$\begin{bmatrix} \dot{x}_1 \\ \dot{x}_2 \end{bmatrix} = \begin{bmatrix} 0 & 1 \\ 0 & 0 \end{bmatrix} \begin{bmatrix} x_1 \\ x_2 \end{bmatrix} + \begin{bmatrix} 0 \\ \beta \end{bmatrix} u \tag{17}$$

$$y = [1 \ 0] \begin{bmatrix} x_1 \\ x_2 \end{bmatrix}$$

as in eqns. 4. Simple calculations shows that

$$\begin{bmatrix} x_1 \\ x_2 \end{bmatrix} = \begin{bmatrix} y \\ \dot{y} \end{bmatrix} = \begin{bmatrix} z_1 \\ -a_1 \sqrt{z_1} + a_2 \sqrt{z_2} \end{bmatrix}$$

i.e.

$$\varphi_z(z) = \begin{bmatrix} z_1 \\ -a_1 \sqrt{z_1} + a_2 \sqrt{z_2} \end{bmatrix}$$

or that $\varphi(\boldsymbol{h})$ is as given in eqn. 2. The inverse mapping from $\boldsymbol{x}$ to $\boldsymbol{z}$ is given by $\phi_z(\boldsymbol{x})$, where

$$\phi_z(\boldsymbol{x}) = \begin{bmatrix} x_1 \\ \left(\frac{x_2 + a_1 \sqrt{x_1}}{a_2} \right) \end{bmatrix}$$

or the mapping from $\boldsymbol{x}$ to $\boldsymbol{h}$ is as given eqn. 5. Further calculation reveals that

$$\psi_z(u, z) = (\alpha_1 u_t + \alpha_2) \sqrt{z_2} + \alpha_3 \left(\frac{z_2}{z_1} - 1 \right) \sqrt{z_1}$$

with

$$\alpha_1 = \frac{2C\beta}{a_2} \quad \alpha_2 = C \left[2a_2 - \frac{a_1^2}{a_2} \right] \quad \alpha_3 = a_1 C$$

or that $\psi(u, \boldsymbol{h})$ is as given in eqn. 3. Here the constant $\beta = 5 \times 10^{-5}$ has been introduced in the model, eqn. 4, to ensure the same order of magnitude of the signals entering the cost function in eqn. 7.

11.2 Constrained predictive control

Consider the linear system

$$\boldsymbol{x}_{t+1} = \boldsymbol{A}\boldsymbol{x}_t + \boldsymbol{B}\boldsymbol{u}_t \tag{18}$$
$$\boldsymbol{y}_t = \boldsymbol{C}\boldsymbol{x}_t$$

where t, $k \in \mathbb{Z}$, and define the cost function

$$J_t = \sum_{k=t}^{\infty} \boldsymbol{x}_k^T \boldsymbol{Q} \boldsymbol{x}_k + \boldsymbol{u}_k^T \boldsymbol{R} \boldsymbol{u}_k \tag{19}$$

which is to be minimised with respect to the constraints

$$\underline{\boldsymbol{b}} \leq \boldsymbol{c}_k \leq \bar{\boldsymbol{b}} \quad \boldsymbol{c}_k, \ \underline{\boldsymbol{b}}, \ \bar{\boldsymbol{b}} \in \mathbb{R}^r \tag{20}$$

where $\boldsymbol{c}_k$ is a vector of constraincd physical quantities which depends linearly on the system states and inputs

$$\boldsymbol{c}_k = \boldsymbol{P}\boldsymbol{x}_k + \boldsymbol{H}\boldsymbol{u}_k$$

The inequalities in condition 20 apply element wise and it is assumed that $\underline{\boldsymbol{b}} \leq 0 \leq \bar{\boldsymbol{b}}$. Since we are in a deterministic framework we will constrain the predictive control actions such that

$$\underline{\boldsymbol{b}} \leq \boldsymbol{P}\hat{\boldsymbol{x}}_{k|t} + \boldsymbol{H}\hat{\boldsymbol{u}}_{k|t} \leq \bar{\boldsymbol{b}} \tag{21}$$

is satisfied (for any $k \geq t$).

Let $\mathbb{F} \subseteq \mathbb{R}^n$ denote the admissible set of states, for which the minimisation of J_t over $\hat{\boldsymbol{u}}_{k|t}$ under the constraints in expr. 21 is feasible and results in a finite cost. This problem is an infinite dimensional constrained optimisation problem, but can bc converted [8], to an equivalent finite dimensional problem in which optimisation is over the sequence of the first κ control moves, $\{\hat{\boldsymbol{u}}_{k|t}\}_t^{t+k}$, only, whereas the remainder are as per the unconstrained LQ optimal state feedback law of eqn. 18.

$$\hat{\boldsymbol{u}}_{k|t} = -\boldsymbol{L}\hat{\boldsymbol{x}}_{k|t} \quad k > t + \kappa$$

In this approach it is necessarily to assume that κ is large enough such that the overall predicted control trajectory is feasible, and thus the computations can become intractable.

To circumvent this difficulty, here, we adapt an alternative formulation following the lines in [18] and rephrase the problem in terms of predicted perturbations on the unconstrained optimal solution. In this framework

$$\hat{\boldsymbol{u}}_{k|t} = \hat{\boldsymbol{v}}_{k|t} - \boldsymbol{L}\hat{\boldsymbol{x}}_{k|t} \tag{22}$$

and the cost function can [2] be expressed as

$$\hat{J}_t = \boldsymbol{x}_t^T \boldsymbol{S} \boldsymbol{x}_t + \sum_{k=t}^{\infty} \hat{\boldsymbol{v}}_{k|t}^T (\boldsymbol{B}^T \boldsymbol{S} \boldsymbol{B} + \boldsymbol{R}) \hat{\boldsymbol{v}}_{k|t} \tag{23}$$

Under the same assumption of feasibility, attention is restricted to a finite number, $\kappa + 1$ of non-zero perturbations for which the cost is as given above but with k running from t to $t + \kappa$.

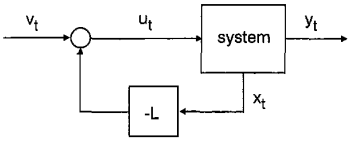

Fig. 12 *Closed-loop system*

Defining

$$\underline{\beta} = \begin{bmatrix} \underline{\boldsymbol{b}} \\ \vdots \\ \underline{\boldsymbol{b}} \end{bmatrix} \quad \bar{\beta} = \begin{bmatrix} \bar{\boldsymbol{b}} \\ \vdots \\ \bar{\boldsymbol{b}} \end{bmatrix} \quad V = \begin{bmatrix} \hat{\boldsymbol{v}}_t \\ \vdots \\ \hat{\boldsymbol{v}}_{t+k} \end{bmatrix}$$

and using the prediction equations

$$\hat{\boldsymbol{x}}_{k+1|l} = \Phi \hat{\boldsymbol{x}}_{k|l} + \boldsymbol{B}\hat{\boldsymbol{v}}_{k|l} \tag{24}$$

and eqn. 22 we may rewrite the constraints in condition 21 as

$$\begin{bmatrix} \boldsymbol{G}_c \\ -\boldsymbol{G}_c \end{bmatrix} V \leq \begin{bmatrix} \bar{\beta} \\ -\underline{\beta} \end{bmatrix} - \begin{bmatrix} \boldsymbol{F}_c \\ -\boldsymbol{F}_c \end{bmatrix} \boldsymbol{x}_t \tag{25}$$

where

$$\boldsymbol{F}_c = \begin{bmatrix} \tilde{\boldsymbol{P}} \\ \vdots \\ \tilde{\boldsymbol{P}}\Phi^{\kappa} \end{bmatrix} \quad \boldsymbol{G}_c = \begin{bmatrix} \boldsymbol{H} & 0 & \cdots & 0 \\ \tilde{\boldsymbol{P}}\boldsymbol{B} & \boldsymbol{H} & \cdots & 0 \\ \tilde{\boldsymbol{P}}\Phi\boldsymbol{B} & \tilde{\boldsymbol{P}}\boldsymbol{B} & \cdots & 0 \\ \ddots & \ddots & \vdots & 0 \\ \tilde{\boldsymbol{P}}\Phi^{\kappa-1}\boldsymbol{B} & \tilde{\boldsymbol{P}}\Phi^{\kappa-2}\boldsymbol{B} & & \boldsymbol{H} \end{bmatrix}$$

for $\tilde{\boldsymbol{P}} = \boldsymbol{P} - \boldsymbol{HL}$.

A direct implementation of this method, which could be referred to as LQ constrained predictive control (LQCPC), would at each instant of time involve the solution of a QP problem with $\kappa+1$ decision variables and $(\kappa+1)r$ constraints. As with optimisation over V this QP problem could be intractable for large values of κ, so we instead use a method which requires very much less computation. This method is referred to as suboptimal constrained predictive control (SCPC).

If the perturbation sequence $\hat{\boldsymbol{v}}^o_{k|t} = 0$ results in feasible trajectories, then the unconstrained LQ optimal feedback law is the solution to the optimisation problem. Let us denote $\boldsymbol{v}^o_{k|t} = 0$ as the LQ perturbation.

Consider the trajectories $\hat{\boldsymbol{v}}_{k|t-1}$, which are the extension to current time of the previous planned perturbation and which, for convenience, will be denoted as the tail. By assumption the tail is feasible, so instead of determining the overall optimal perturbation sequence $\hat{\boldsymbol{v}}^*_{k|t}$ each time, we will find a pertubation sequence, which is a linear interpolation between the tail and the LQ perturbation, i.e.

$$\hat{\boldsymbol{v}}_{k|t} = \alpha_t \hat{\boldsymbol{v}}_{k|t-1} \quad \text{for } k \geq t$$

and $0 \leq \alpha_t \leq 1$. This inserted in the cost function in eqn. 23 and in the constraints in expr. 25, results in a univariate (and hence very undemanding) minimisation problem in $\alpha_t \in [0; 1]$ subject to the constraints

$$\begin{bmatrix} \boldsymbol{G}_c\tilde{V} \\ -\boldsymbol{G}_c\tilde{V} \end{bmatrix} \alpha_t \leq \begin{bmatrix} \tilde{\beta} \\ -\underline{\beta} \end{bmatrix} - \begin{bmatrix} \boldsymbol{F}_c \\ -\boldsymbol{F}_c \end{bmatrix} \boldsymbol{x}_t \tag{26}$$

where

$$\tilde{V} = \begin{bmatrix} \hat{\boldsymbol{v}}_{t|t-1} \\ \vdots \\ \hat{\boldsymbol{v}}_{t+k|t-1} \end{bmatrix}$$

This problem requires much less computation each instant of time.

Initially, at $t=0$, we do not have the tail of a previous planned trajectory, but must directly determine a feasible solution $\hat{\boldsymbol{v}}_{k|0}$. A convenient way of doing this is to determine the initial perturbation sequence as the sequence that minimises the cost function

$$\bar{J} = \sum_{k=0}^{\infty} \boldsymbol{c}_k^T \bar{\boldsymbol{Q}} \boldsymbol{c}_k + \boldsymbol{v}_k^T \bar{\boldsymbol{R}} \boldsymbol{v}_k \tag{27}$$

where the mix of the two terms can be so designed as to reach a compromise between constraints satisfaction (which requires a large $\bar{\boldsymbol{Q}}$) and deviation away from the LQ optimal (which can be required if $\bar{\boldsymbol{R}}$ is chosen to be large). If $\boldsymbol{K}$ is the solution to the LQ-problem in eqns. 24 and 27, then the initial perturbation sequence can be expressed as

$$\hat{\boldsymbol{v}}_{k|0} = -\boldsymbol{K}(\Phi - \boldsymbol{BK})^k \boldsymbol{x}_0$$

Furthermore, since

$$\hat{\boldsymbol{v}}_{k|t} = -\boldsymbol{K}(\Phi - \boldsymbol{BK})^k \boldsymbol{x}_0 \prod_{i=0}^{t} \alpha_i$$

and $\alpha_i \leq 1$ for $i \geq 0$, the contribution of the initial perturbation trajectory is gradually reduced as feasibility permits α_t to decrease.

Another alternative way, which has been proven advantageous in [13] and [7], is to determine $\hat{\boldsymbol{v}}_{k|0}$ as a mean level control, i.e. a detuned LQ control, of the system in eqn. 24.

Assuming that the initial perturbations sequence is feasible, the resulting predictive control law based on the interpolation algorithm i.e. the algorithm which minimises α subject to condition 26, can be proven to be asymptotically stable.

11.3 Computational efficiency

In order to investigate the efficiency of SCPC, the algorithm has been applied to a number of systems with a unity steady-state gain. Both SCPC and the QP-based LQCPC were applied and the results are summarised in Table 1.

Table 1. List of experiments

Experiment	System	Jump	Period length	Ratio
1	$1/(\tau_1 s+1)$	1	6	41.4
2	$1/(\tau_2 s+1)$	1	12	51.4
3	$1/((\tau_1 s+1)(\tau_2 s+1))$	1	18	61.0
4	$\omega^2/(s^2+2\mu\omega+\omega^2)$	1	18	61.2
5	$\omega^2/((\tau_1 s+1)(s^2+2\mu\omega+\omega^2))$	1	20	60.8
6	$1/((\tau_1 s+1)(\tau_2 s+1))$	1.9	67	225.4

'Jump' is the size of the set point change, 'period length' is the length of the period in which the constraint is active and 'ratio' is the ratio between the required floating point operations in the LQCPC and SCPC

The systems are in an observer canonical form and are sampled with $T=1$ s. Their transfer functions are listed in Table 1. The control objective is given by $\boldsymbol{Q}=\boldsymbol{C}^T\boldsymbol{C}$, $R=0.01$. The constraint is a limited control $|u_t| \leq 2$, i.e. $P=0$ and $H=1$. In the SCPC algorithm, the initial feasible perturbation sequence is determined with $\boldsymbol{Q}=1$ and $\bar{\boldsymbol{R}}=0$. The length of the horizon in both algorithms was $\kappa=35$. The responses (for output y_t, set point w_t and control input u_t) are quite similar to the responses in Fig. 5, except for the fact that the systems are different. The constants used in the simulations were $\tau_1=10$ s, $\tau_2=20$ s, $w=2\pi/\tau_3$ where $\tau_3=180$ and $\mu=0.1$.

As is clear from Table 1, LQCPC requires a much higher computational demand, especially in situations where the constraints are active for long periods of time.